Proceedings of the 2007 IEEE/RSJ International
Conference on Intelligent Robots and Systems
San Diego, CA, USA, Oct 29 - Nov 2, 2007

Energy-Field Reconstruction For Haptic-Based Molecular Docking Using Energy Minimization Processes

Bruno Daunay[1], Alain Micaelli[2], Stéphane Régnier[3]

[1,3]Laboratoire de Robotique de Paris, CNRS - UPMC, BP 61, 92265 Fontenay Aux Roses, France
[2]CEA-LIST, 18 route du Panorama, BP6, 92265 Fontenay Aux Roses, France

daunay@robot.jussieu.fr, alain.micaelli@cea.fr, regnier@robot.jussieu.fr

***Abstract*— This paper presents a new method allowing haptic feedback in molecular docking simulations using a minimization process. These simulations, classically used by the pharmaceutical industry, for example Sanofi-Aventis, are based on the energy description of atoms to estimate the interactions between a ligand and a protein. The main drawback is that forces and torques cannot be calculated by the means of a simple derivation. The proposed method is to locally build an energy model, the shape of which is correctly predetermined, depending on parameters to be estimated, themselves functions of the energy of the interatomic interactions and of the displacement of the haptic device. The interaction's wrench can be obtained using an analytic derivation of the energy model. The molecular simulator does not need to be optimized or modified, only the calculated interaction energy is used to build a model which will interact with the haptic device. This new method can then be used with any force field using a minimization process, ensuring stable manipulation, and a low-force dynamic, therefore allowing comprehensive and stable force feedback.**

I. Introduction

Drugs are made of small molecules (ligands), which interact with proteins in order to inactivate them through a specific pocket (binding site or active site). The computational process of searching for a ligand that is able to fit the binding site of a protein is called molecular docking. The conformation of the ligand into the binding site has the lowest potential energy. The only information provided by the software used during the simulation, are a visual return of the conformation of the molecules and the value of the energy involved. Because of the relatively low docking success rates for fully automated algorithms, including a human operator in the loop appears as a solution [1] [2].

Interactive haptic feedback for molecular docking can give additional information on the behavior of the forces present inside the receptor. The operator would then be able to feel the repulsive or the attractive areas and define the best geometry of the ligand that maximizes the interaction energy [3]. This is in order to discriminate the geometry of the best potential candidates after virtual screening simulations, in order to conceive efficient drugs.

The aim of our work is not to optimize the molecular simulators (as proposed in some other works [4], [5], [6]) but to conceive a method that takes into consideration their specificities. Indeed, the pharmaceutical engineers use software which is not real-time but which describes the interatomic interactions very precisely. They would like to use them with haptic feedback without having to modify them. Moreover, for their research, they use several force fields, each being specific to a molecular property.

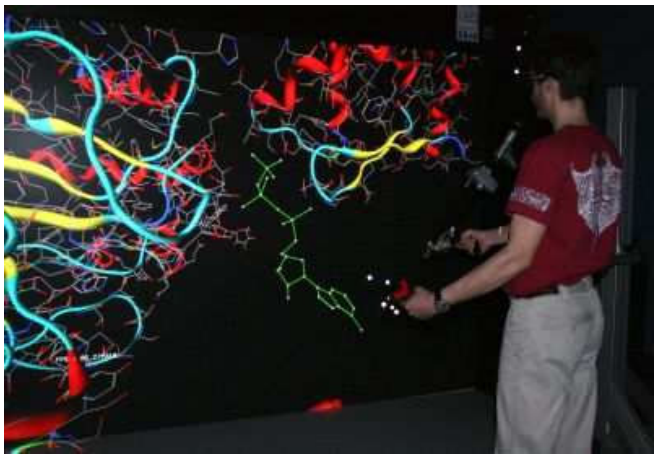

Fig. 1. Manipulation scene. The ligand (green molecule) has to be moved through the protein to the binding site. The protein will search for a stable conformation during docking.

Starting from pharmaceutical engineers' needs, that is to say, where several force fields have to be minimized, interatomic interactions have to be described with a force field depending on the properties of proteins, we developed a method enabling the forces and the torques to be felt during 6 DOF molecular docking, using any molecular simulator based on a force field minimization process, moreover avoiding the need of particular molecular simulation knowledge. The minimized interaction energy between the ligand and the protein is locally approximated by an energy equation containing terms to evaluate, functions of the displacement of the haptic device and the profile of the interaction energy, from which an analytic derivation is known, allowing the interaction forces and torques to be obtained. The haptic device then interacts with the new model, itself updated as soon as a new energy is calculated, making the haptic interaction to be in real time, even if the molecular simulation is not.

This article is structured as follows: the first paragraph describes the force field and the simulation we usually use

in order to evaluate both the interaction energy between the ligand and the protein, and the conformational changes of these two molecules. The second paragraph describes and validates the method used to evaluate the parameters of the built energy that approaches the real energy. The forces profile obtained during a docking simulation using a wave variable coupling method [7] are then exposed.

II. Force field model and Simulation method

A. Force field

The model we use, which is described below, is called MMFF94 [8]. A general equation of total energy, such as (1), includes terms for bond stretching (E_{Bond}), angle bending (E_{Angle}), torsion ($E_{Torsion}$), and non-bonded interactions such as electrostatic (E_{Elec}) and Van der Waals energies (E_{VdW}).

$$E_{Total} = E_{Bond} + E_{Angle} + E_{Torsion} + E_{Elec} + E_{VdW} \quad (1)$$

Bond stretching and angle bending energies allow a flexible geometry. The simplest approach, based on the fact that most bonds are near the minimum of their energy, employ a quadratic term to model bond stretching and angle bending energies, as in (2) and (3).

$$E_{Bond} = \sum k_{Bond}/2(l - l_0)^2 \quad (2)$$

$$E_{Angle} = \sum k_{Angle}/2(\theta - \theta_0)^2 \quad (3)$$

Where k_{Bond} and k_{Angle} (stiffness of the bond and of the angle) are experimentally obtained. l, l_0 and θ, θ_0 are respectively actual and ideal bond lengths and actual and ideal bond angles. In fact, these energy terms are more complicated. For bond energies, cubic terms are introduced as angle energies [9].

The torsion energy expression is represented by a Fourier series expansion which, as shown in (4), includes three terms.

$$E_{Torsion} = 1/2 \sum [\, V_1(1+\cos\phi) + V_2(1-\cos 2\phi) + V_3(1+\cos 3\phi)\,] \quad (4)$$

Where V_1, V_2 and V_3 are torsional barriers specified for the pair of atoms around which the torsion occurs. ϕ is the torsion angle (the rotation angle around the bond between the second and third atom in any serially connected four atoms).

Vand der Waals interactions are described with the "Buffered 14-7" form [10]. The form of the potential is shown in (5). R_{ij} corresponds to the distance between atom i and atom j.

$$E_{VdW_{ij}} = \varepsilon_{ij} \left(\frac{1.07 R_{ij}^*}{R_{ij} + 0.07 R_{ij}^*} \right)^7 \left(\frac{1.12 R_{ij}^{*\,7}}{R_{ij}^7 + 0.12 R_{ij}^{*\,7}} - 2 \right)^7 \quad (5)$$

This form is used with an expression that relates the minimum energy separation R_{ii}^* (which can be assimilated close to the Van der Waals radius of atom i) to the atomic polarizability α_i (6), with specially formulated combination rules (7, 8), and with the potential depth ε_{ij} describing the minimum energy for a given atomic pair i and j.

$$R_{ii}^* = A_i \alpha_i^{1/4} \quad (6)$$

Where A_i is an experimentally defined constant.

$$R_{ij}^* = 1/2(R_{ii}^* + R_{jj}^*)(1 + 0.2(1 - \exp(-12\gamma_{ij}^2))) \quad (7)$$

$$\gamma_{ij} = (R_{ii}^* - R_{jj}^*)/(R_{ii}^* + R_{jj}^*) \quad (8)$$

MMFF94 uses the buffered coulombic form as an electrostatic interaction.

$$E_{Elec_{ij}} = 332.0716 q_i q_j / \left(D(R_{ij} + \delta)^2 \right) \quad (9)$$

Where q_i and q_j are partial atomic charges of atoms i and j, R_{ij} is the internuclear separation. $\delta = 0.05$ Å is the electrostatic buffering constant and D the dielectric buffering constant.

B. Simulation

Energy minimization consists in finding a set of atomic coordinates that corresponds to a local minimum of the molecular energy function (it clearly appears that the simulation should take a long time to reach the global minimum). This is done by applying large-scale non-linear optimization techniques to calculate a conformation (near the initial geometry) for which the forces on the atoms are null [11].

Because the simulation is entirely based on the energy description of the interatomic interactions, the forces are not able to be directly obtained from the model unlike for simulations of molecular dynamics. The next paragraph describes the method we use to overcome this problem, letting the operator interact with a predicted energy easily convertible into forces and torques.

III. From an energy description of a force field to force feeling

A. Simple approach

As described in paragraph II, the force field describing the protein's behavior uses the interaction energy. Consequently, a derivation of this interaction energy in the three space directions is made as a first approximation (highly approximate formulation of the forces starting from the energy, only allowing us, at first, to understand the profile of the forces during a docking procedure):

$$W_i^{\text{Simulation}} = \frac{E_i - E_{i-1}}{x_i^{nano} - x_{i-1}^{nano}} \quad (10)$$

where i is the iteration number and x^{nano} the position and orientation of the interface in the nano world. A singularity will appear if the interface displacement between step i and $i+1$ is null. Then, the force/torque sent to the interface is arbitrarily set to the previous force/torque.

Derivating the energy relative to the variation of the position or the angle variation of the haptic device is not a good way of obtaining the interaction's wrench. In fact, the minimization of the force field provides an energy that is not directional. The results are not the exact wrench of the interaction efforts. The forces profile obtained using this method is shown in Fig. 2. It is clear that this forces profile cannot be well interpreted from a haptic point of view. The need for a smooth and correct forces profile means a different

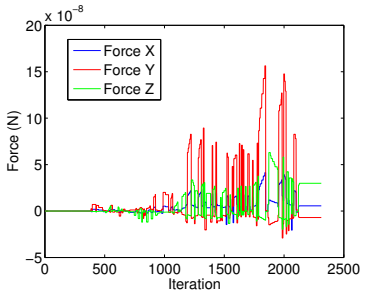

Fig. 2. Force profil around the minimized ligand position along the x, y and z axes using the simple derivation method.

method must be adopted. Knowing that directional energy cannot be calculated from classical molecular simulators, we decided to calculate an energy field in which each term allows an analytical solution for the forces and the torques to be obtained.

B. Approximation of the energy

Starting from the hypothesis that locally, the energy field has no large variations for a specific protein conformation, to reconstruct an energy field depending on parameters to identify, from which the derivation has no singularity, appears to be a solution for easily converting the energy provided by the minimization process into a wrench.

The principle of our second method is to approach the energy calculated by the minimization process ($E^{measure}$) by a potential containing two terms (depending on parameters - here represented by θ -) and representing the forces and the torques of the interaction ($\widehat{E}(p,R,\theta)$) so that the potential gradient at each of the ligand's position p and orientation R is equal to the interaction forces and torques ($W(p,R)$):

$$\nabla_{(p,R)}\widehat{E}(p,R,\theta) = W(p,R)\ \forall(p,R) \tag{11}$$

This new potential has to be compared to the interaction energy through a root mean square method, determining its parameters at each of the ligand's position and orientation.

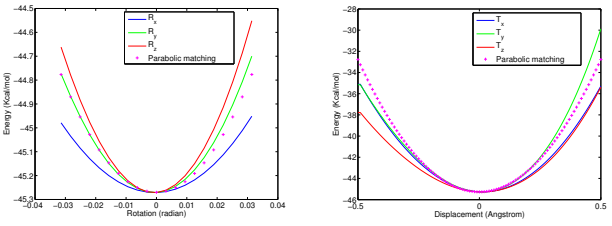

(a) (b)

Fig. 3. Energy field evaluation between the ligand (biotin) in the minimized streptavidin complex. (a) Rotation of the ligand around its equilibrium position. (b) Translation of the ligand around its equilibrium position. A comparison with a quadratic function is made, validating the choice of quadratic terms for the predicted energy.

As shown on Fig. 3, the interaction energy field looks like a polynomial function (quadratic function). The shape of the function to be estimated must approach the polynomial function in order to ensure the algorithm's convergence. Let us consider the function described in (12) as a potential to be evaluated. Let i be the current object frame and e the equilibrium one. Then:

$$\widehat{E}_i(p,R,k_t,p_e,g_0,R_e) = \frac{1}{2}k_t||^i p - ^i p_e||^2 - g_0 tr(^iR^t R_e) + c \tag{12}$$

where p is the position of the ligand's center of mass (haptic device position), R the haptic device rotation, k_t and g_0 are arbitrarily set as spring constants, they should be chosen as a diagonal matrix in order to provide different gains according to the displacement's direction (as shown on Fig. 3, translations and rotations have different values according to the displacement's axes). p_e and R_e are the equilibrium position and orientation of the estimated potential, and c a positive constant to be estimated (it is set as zero initially). The function has two terms (considering a null constant), their derivation allowing respectively the forces and the torques to be found. Finding the estimated potential parameters, requires solving the problem described below:

$$\min_{\theta}\sum||E^{measure} - \widehat{E}(p,R,\theta)||^2 = \sum\varepsilon \to 0 \tag{13}$$

where θ represents the parameters set (k_t, p_e, g_0, R_e), $E^{measure}$ the interaction energy provided by the minimization process, $\widehat{E}(p,R,\theta)$ the estimated energy calculated from (12) and ε represents the error between the estimation and the measure. Considering that $\widehat{E}(p,R,\theta)$ does not depend linearly on its parameters, (13) has to be linearized:

$$E^{measure}_{i+1}(p,R) = \widehat{E}_{i+1}(p,R,\theta) + \frac{\partial E_{i+1}(p,R,\theta)}{\partial\theta}\delta\theta \tag{14}$$

where i represents the step number. The measured potential can then be expanded, in order to evaluate the estimated gradient of the potential regarding its parameters θ.

$$\begin{aligned} E_{i+1} = \widehat{E}_{i+1} \quad &+ \quad \frac{1}{2}||^{i+1}p - ^{i+1}p_e||^2\delta k_t - tr\left(^{i+1}R^t R_e\right)\delta g_0 \\ &- \quad k_t(^{i+1}p - ^{i+1}p_e)^t\delta p_e \\ &+ \quad 2g_0\left[as\left(^{i+1}R^t R_e\right)^{V\,t}\right]\delta\theta_e \end{aligned} \tag{15}$$

$as\left(^{i+1}R^t R_e\right)^V$ is the antisymmetric part of the equilibrium rotation matrix, written as a vector. The predicted gradient is then written as:

$$\begin{aligned} \nabla_\theta\widehat{E}_{i+1} = \Big[\quad &+ \quad \frac{1}{2}||^{i+1}p - ^{i+1}p_e||^2, -tr\left(^{i+1}R^t R_e\right), \\ &- \quad k_t(^{i+1}p - ^{i+1}p_e)^t, \\ &+ \quad 2g_0\left[as\left(^{i+1}R^t R_e\right)^{V\,t}\right] \quad \Big] \end{aligned} \tag{16}$$

Equation 14 could then be rewritten, taking into consideration (16):

$$\begin{bmatrix} \nabla_\theta\widehat{E}(i,p(i),\theta(i-1)) \\ \nabla_\theta\widehat{E}(i-1,p(i-1),\theta(i-2)) \\ \vdots \\ \nabla_\theta\widehat{E}(i-m,p(i-m),\theta(i-m-1)) \end{bmatrix} \begin{bmatrix} \delta k_t \\ \delta p_e \\ \delta g_0 \\ \delta R_e \end{bmatrix} =$$

$$\begin{bmatrix} E^m(i,p(i)) - \widehat{E}(i,p(i),\theta(i-1)) \\ E^m(i-1,p(i-1)) - \widehat{E}(i-1,p(i-1),\theta(k-2)) \\ \vdots \\ E^m(i-m,p(i-m)) - \widehat{E}(i-m,p(i-m),\theta(i-m-1)) \end{bmatrix} \quad (17)$$

Each parameter can be updated from 17 and 18, using a recursive or not, weighted or not, root mean square method.

$$\theta(i+1) = \theta(i) + \delta\theta \quad (18)$$

That is to say,

$$\begin{cases} k_t(i+1) &= k_t(i) + \delta k_t \\ p_e(i+1) &= p_e(i) + \delta p_e \\ g_0(i+1) &= g_0(i) + \delta g_0 \\ R_e(i+1) &= R_e(i) exp^{[\delta R_e]} \end{cases} \quad (19)$$

The larger the size of the matrix of the predicted gradient, the more precise the estimation of the parameters is. However the calculation time needed for the inversion of the matrix will also be higher. The size of the matrix will then have to be a compromise between the short computational time needed for real-time haptic feedback and the precision of the model.

C. Limits

This last algorithm step (19) allows updated values for the approximated energy to be obtained. This estimation should provide a close representation of the energy field provided that the shape of the estimator is not too far remote from the measured field. The algorithm also depends on initial conditions and on the excitation type. For initial conditions that are very remote from the solution, the algorithm will take a long time to converge. An estimation of the solution could be a good way of ensuring the convergence, knowing that the forces are calculated from the estimation. This implies ensuring the convergence at each time step. The estimated gradient matrix shape is important. Updated parameters are provided by its inverse. A guarantee of its existence is that there are no linear combinations of the lines. In other words, during the ligand manipulation, if there is no displacement setting, the ligand has to be moved randomly around its actual position. First to prevent the estimated gradient to be uninvertible and secondly to enrich the parameters ensuring a good force feedback.

D. Simulations

The goal of the simulation is to simulate a random energy field that would be predicted but with a shape near to the solution in order to avoid algorithm divergence.

1) Approximation of the energy regarding translation: Consider as a force field to be approximated that described below (20), and its approximated function (21)

$$E^{measure} = x^2 + y^2 + z^2 - 1 \quad (20)$$

$$\widehat{E} = \tfrac{1}{2} k_t ||p - p_e||^2 - 1 \quad (21)$$

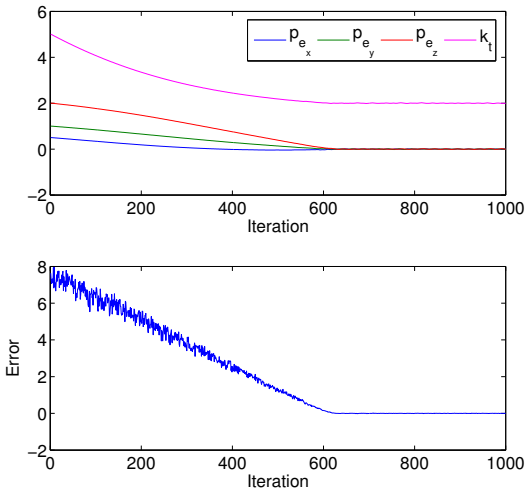

Fig. 4. Results obtained after having approximated the translation energy field. The first graph presents the parameters estimations and the second, the error between the estimated and the measured energy.

$\widehat{E}$ is calculated from $E^{measure}$ considering random real positions. In the case of docking, these positions will be those of the haptic device.

Starting from initial conditions ($p_e = [0.5, 1, 2]$ and $k_t = 5$) close to the desired position, the algorithm converges to the solution in about 600 iterations (Fig. 4). This number may vary considering a constant α used to moderate the parameters' updates (22).

$$\theta(i+1) = \theta(i) + \delta\theta/\alpha \quad (22)$$

This parameter α has to be carefully chosen. If it is too high, the algorithm will converge in too many iterations making good energy approximation impossible during the ligand manipulation, as the shape of $E^{measure}$ also varies. If it is too small, the algorithm will converge, faster but the parameters will oscillate near the equilibrium value, inducing varying forces for a constant energy field. Finally, according to the results, $E^{measure}$ is approximated by $\widehat{E}$ with the parameters $k_t = 2$, $p_{e_x} = p_{e_y} = p_{e_z} = 0$. In fact, $E^{measure} = \widehat{E} = (1/2)2((x-0)^2 + (y-0)^2 + (y-0)^2) - 1$. This trivial example clearly illustrates the principle of this method.

2) Approximation of the energy regarding rotations: All real and estimated rotations have to be written in the same frame. For simulation needs, the estimated energy and the real energy are expressed in terms of rotation (23 and 24).

$$E^{measure} = -g_{0_{nom}}(\mathrm{tr}(R^t R_{e_{nom}}) - 3) \quad (23)$$

$$\widehat{E} = -g_0(\mathrm{tr}(R^t R_e) - 3) \quad (24)$$

Where R is a random rotation matrix, R_e the estimated equilibrium rotation, $g_{0_{nom}}$ the value g_0 will tend towards to, as R_e towards to $R_{e_{nom}}$. In order to build the estimated gradient matrix, $\widehat{E}$ had to be derivated relative to its parameters g_0 and R_e. In the case of such an energy, the gradient is

expressed as (25).

$$\nabla_\theta \widehat{E} = \left[-\left(\mathrm{tr}(R^t R_e) - 3\right), 2g_0 \left(as(R^t R_e)^{Vt}\right)\right] \qquad (25)$$

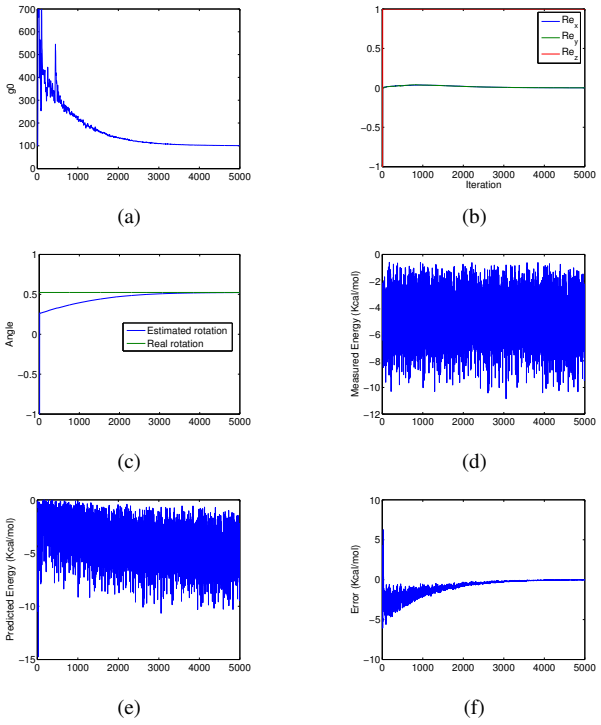

Fig. 5. Results obtained after having approximated the rotation energy field.

Fig. 5(a) shows the convergence value for the parameter g_0. The initial conditions for the simulation from which the results were obtained were random g_0 and R_e. $g_{0_{nom}}$ was set at 100 and $R_{e_{nom}}$ represented a $\pi/6$ rotation along the z axis. As shown in Fig. 5(b) and Fig. 5(c), the estimation converges to the desired value. First, we can observe a rotation along the z axis (represented values are the normalized rotation vector), and second that the angle converges to $\pi/6$. Fig. 5(d), 5(e) and 5(f) respectively represent the real energy calculated from the random rotation matrix R (in practice, these values will be the haptic device's ones), the estimated energy and the predicted error between the measure and the prediction. At the end of the simulation, the real energy field is approximated by the one we built with the parameters then updated. It is clear that the convergence speed depends on the real energy field to be estimated and on the parameter α introduced in (22). The shape of the function of the predicted energy has to be close to the real shape. Inside a protein, with the force field described in the previous paragraph, and considering Fig. 3, we may suppose that we have a good prediction function. We use $(\mathrm{tr}(R^t R_e) - 3)$ rather than $(\mathrm{tr}(R^t R_e))$ to predict the rotation because the energy has to tend toward zero if the equilibrium rotation tends toward the identity matrix.

The method is proved convergent in the case of translations and rotations. Starting from these observations, we implemented the method in our molecular simulator. The predicted energy's shape is then the sum of the translation term (21) and the rotation term (24).

E. Application

In order to feel the docking forces, the force field has to be approximated first. The operator will then interact with the approximated model, it being updated at each time step.

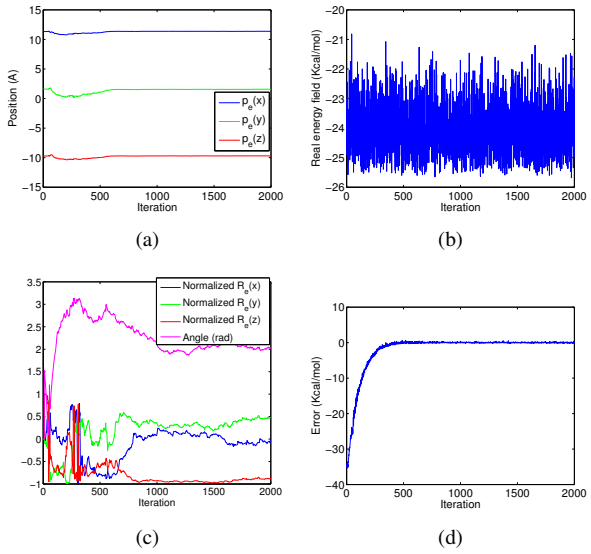

Fig. 6. Approximation of the force field in a minimized streptavidin complex. (a) Position of the potential minimum, (b) Measured interaction energy, (c) Orientation of the potential minimum, (d) Estimation error.

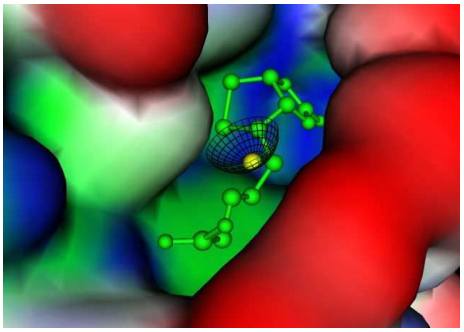

Fig. 7. Graphical interpretation of Fig. 6. The yellow sphere represents the predicted interaction potential minimum (obtained from 6(a)) itself represented by the colored surfaces. The potential orientation is determined by the orientation of the half sphere (obtained from 6(b)).

Fig. 7 is the graphical representation of the simulation for which the results are shown on Fig. 6. The interaction energy has to be approximated by a polynomial function. Graphically, the interaction surface can be approximated by the yellow sphere and the orientation of the half sphere. Then, the forces felt correspond to the distance between the real haptic device's position and the yellow sphere, and the torques correspond to the orientation difference between the haptic device's rotation and the half sphere (in

an approximate way). For each ligand manipulation, all the parameters of the model are updated to obtain the potential minimum position and its orientation knowing that forces and torques are obtained regarding these parameters.

F. Interaction's wrench calculation

Once the interaction energy is predicted, the forces are calculated taking into consideration its gradient. The new gradient is obtained not from the parameters but from the position and the orientation of the haptic device. Unlike the simple approach, the forces obtained are defined whatever the haptic device's displacement is. This is done as follows:

$$W = \left[k_t(p - p_e), 2g_0\left(as(R^t R_e)^{Vt}\right)\right] \tag{26}$$

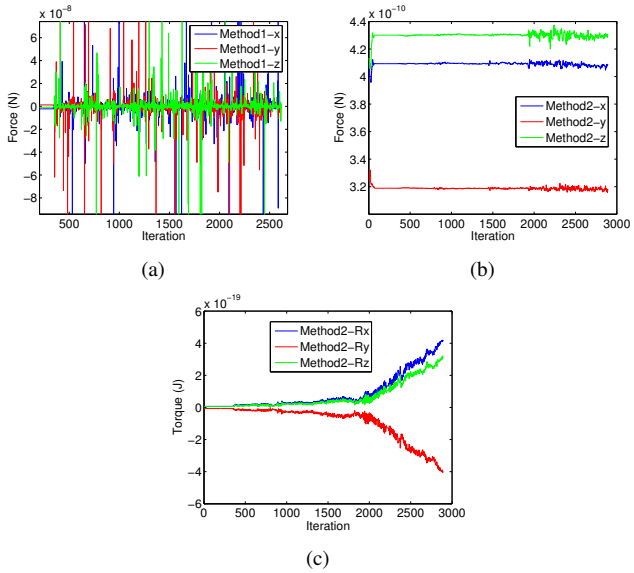

Fig. 8. Forces and torques during the ligand's manipulation inside the active site. (a) Forces calculated from the first method, (b) Forces obtained after having approximated the energy field, (c) Torques calculated from the second method.

Fig. 8 shows the forces and torques obtained during a ligand manipulation inside the active site using the wave variable coupling presented in [7]. Fig. 8(a) represents the forces profile obtained from the first method. The forces' amplitude seems very high. This result has to be compared to the Fig. 8(b). In fact this last graph shows the forces we obtained after having made the energy approximation. It is clear that, because of the small variation of the parameters set, the forces profile looks smoother, therefore hapticaly comprehensive. The torques are represented on Fig. 8(c).

The interesting results are that, unlike those obtained with the first method, the forces inside the active site seem to vary very little (taking into consideration that the operator makes little displacements). The forces inside the active site are well depicted and do not seem as unstable as those obtained from a simple derivation. Considering this method, a parallel between the micro world and the macro world can be established. Indeed, research on the force factor problem can be lead unlike with the first method in which the forces are too unstable.

IV. CONCLUSIONS AND FUTURE WORKS

A. Conclusions

In this paper, a method for haptic-based molecular docking using minimization processes is presented. Starting from initial observations - simulation based on the energy and high force amplitudes in our first method - we have implemented a new method that allows the real forces present inside the active site to be obtained. In the first stage, the interaction energy was basically derivated, thus introducing singularities and high force amplitudes. This problem is solved in the second stage. The interaction energy provided by the minimization process is approximated by an energy model containing parameters to be evaluated, and allowing, whatever the displacement is, the real forces and torques that look stable in this particular case to be obtained. The second method allows a stable simulation to be obtained, making it possible for the operator to interprete the micro forces.

B. Future work

The interaction energy profile is determined around the ligand position. This is a very time-consuming method because several estimations of parameters have to be made in order to provide a very precise estimated energy. Another approach leads to pre-calculating the approximated interaction energy in a desired conformation around a predetermined grid, and then locally updating the model during the manipulation and the conformational change of the protein.

REFERENCES

[1] M. Ouh-Young, M. Pique, J. Hugues and al., Using a manipulator for force display in molecular docking, proc. of International Conference on Robotics and Automation, 1988, pp. 1824-1829.

[2] M. Ouh-Young, D. Beard, F. P. Brooks Jr, Force display performs better than visual display in simple 6DOF docking task., proc. of International Conference on Robotics and Automation, 1989, pp. 1462-1466.

[3] E. Subasi C. Basdogan, A New Approach to Molecular Docking in Virtual Environments with Haptic Feedback, proc. of EuroHaptics, 2006, pp. 141-145

[4] K. Kazerounian, From Mechanisms and Robotics to Protein Conformation and Drug Design, *Proc of ASME*, vol. 126, 2004, pp. 40-45.

[5] J. Cortés, T. Siméon and al., A path planning approach for computing large-amplitude motions of flexible molecules, *Bioinformatics*, vol. 21, 2005, pp. i116-i125

[6] S. Morin, S. Redon, A Force-Feedback Algorithm for Adaptive Articulated-Body Dynamics Simulation, In Proceedings of IEEE International Conference on Robotics and Automation, 2007

[7] B. Daunay, A. Micaelli, S. Régnier, 6 DOF haptic feedback for molecular docking using wave variables, In Proceedings of IEEE International Conference on Robotics and Automation, 2007

[8] T.A. Halgren, Merck molecular force field. IV. Conformational energies and geometries, *J. Comp. Chem.*, vol. 17, 1996, pp. 587-615.

[9] T.A. Halgren, Merck molecular force field. I. Basis, Form, Scope, Parametrization, and Performance of MMFF94, *J. Comp. Chem.*, vol. 17, 1996, pp. 490-519.

[10] T.A. Halgren, Representation of van der Waals (vdW) Interactions in Molecular Mechanics Force Fields: Potential Form, Combination Rules, and vdW Parameters, *J. Am. Chem. Soc.*, vol. 114, 1992, pp. 7827-7843.

[11] P.E. Gill, W. Murray, M.H. Wright, Practical Optimization, Academic Press, London, 1981.